



Synthesis and characterization of poly(vinyl alcohol)-acid salt polymer electrolytes

Reda Khalil^{1,2,*}, Eslam Sheha², Taha Hanafy^{1,†}, and Omar Al-Hartomy¹

¹Physics Department, Faculty of Science, Tabuk University, 71421, KSA

²Physics Department, Faculty of Science, Benha University, Benha, 13518, Egypt

ABSTRACT

A solid acid membranes based on poly(vinyl alcohol) (PVA), magnesium bromide (MgBr_2) and phosphoric acid (H_3PO_4) were prepared by a solution casting method. The morphological, X-ray and electrical properties of the $(\text{PVA})_{(1-x)}(\text{MgBr}_2)_{x/2}(\text{H}_3\text{PO}_4)_{x/2}$ solid acid membranes where $x = 0.0, 0.1, 0.2, 0.3$ and 0.4 wt% were investigated. The PVA polymer electrolyte directly blended with acid salt shows improvement in ionic conductivity and transport properties. The maximum ionic conductivity value of PVA/acid salt polymer electrolyte with $x = 0.40$ wt% of acid salt is around $1.64 \times 10^{-4} \text{ S cm}^{-1}$ at 20°C and the ionic transport number (t^+) is in the range of 0.98 – 0.99 . In this work, the data shows that the $(\text{PVA})_{(1-x)}(\text{MgBr}_2)_{x/2}(\text{H}_3\text{PO}_4)_{x/2}$ solid acid salt membrane is promising for intermediate temperature phosphoric acid fuel cell applications.

Keywords: Polymer Electrolytes, Ionic Conductivity, Phosphoric Acid, Dielectric Properties.

1. INTRODUCTION

In recent times extensive investigations on solid polymer electrolytes (SPE) have been in progress in view of their potential applications in solid state electrochemical cells.^(1–3) The solid polymer electrolytes (SPE) have become the area of wide variety of fundamental and technological applications such as solid state batteries, fuel cells, double layer capacitors, sensors, electrochemical display devices, etc.^(4–8) The one of the important components in rechargeable batteries and fuel cells devices is the ionic conductor (electrolyte). Due to some special properties, like good mechanical, simple preparation in different forms, good electrode–electrolyte contact and adhesive properties⁽⁹⁾ solid polymer electrolytes (SPEs) have emerged as important ionic conducting materials. One of the attracted polymer electrolyte is proton conducting polymer due to their promising application in

battery and fuel cells. Most proton-conducting polymers depend on their water content, which limits their application. In order to overcome those limitations, a number of studies have been performed to produce novel polymer-based materials that can transport protons under anhydrous conditions. In this context, phosphoric acid based systems are widely studied for that because of its extensive self-ionization and low acid dissociation constant pKa. PVA was used as host polymers that keep phosphoric acid in their matrix and proton transport is mainly provided by phosphoric acid units via structure diffusion where the transference number of proton is close to unity.^(10,11)

Although several homogeneous polymer electrolytes were reported in earlier studies,^(12–15) phosphoric acid doped polybenzimidazole (PBI), showed better physicochemical properties and promising fuel cell performance.^(16–20) Although high proton conductivity can only be achieved at higher acid compositions, dopant exclusion is an important drawback during prolonged usage in fuel cells. Therefore, our work has been driven by a desire to develop a radically new, alternative proton-conducting electrolyte (or membrane) that is based on

* Author to whom correspondence should be addressed.
Emails: rkhailil@fsc.bu.edu.eg, redakhalil67@gmail.com

† Present address: Physics Department, Faculty of Science, Fayoum University, El Fayoum, Egypt.

compounds whose chemistry and properties are intermediate between those of a normal acid, such as H_3PO_4 , and a normal salt, such as NaBr_2 and not a hydrated polymer (solid acid). Thus, membranes will be developed, in which a solid acid salt is embedded in PVA matrix, with the polymer providing mechanical support and enhancing chemical stability. In this study, an attempt has been made to prepare the polymer electrolytes based on PVA complexed with $\text{MgBr}_2/\text{H}_3\text{PO}_4$ at different concentrations expect to use it in fuel cell application. Another approach to the development of proton-conducting membranes is to combine the functions of the Hydroquinone (HQ) and the proton solvent in a single molecule. Such molecules must be amphoteric in the sense that they behave as both a proton donor (acid) and proton acceptor (base), and they must form dynamical hydrogen bonds. Also HQ plays a major role as a reducing agent for bromine and improving the chemical stability of the matrix. In similar study, the results of addition of HQ to $(\text{PVA})_{0.7}$, lithium bromide $(\text{LiBr})_{0.3}$, sulfuric acid $(\text{H}_2\text{SO}_4)_{2.9}$ and 2% (w/v) ethylene carbonate, revealed that, the thermal stability and electrical conductivity of the samples improve on increasing the HQ doping. The film doped with 4 wt% HQ exhibits maximum conductivity was found to be 1.75×10^{-3} S/cm at room temperature.⁽²¹⁾ In the present work, 0.4% (w/v) HQ and 2% (w/v) ethylene carbonate which used as plasticizer were added to $(\text{PVA})_{(1-x)}(\text{MgBr}_2)_{x/2}(\text{H}_3\text{PO}_4)_{x/2}$ membrane to improve the thermal and structural properties. Upon the above considerations, an attempt has been made to synthesis a broad range of $(\text{PVA})_{(1-x)}(\text{MgBr}_2)_{x/2}(\text{H}_3\text{PO}_4)_{x/2}$ polymer composite and conductivity measurements, surface morphologies, and structure of the membranes were investigated. Effects of acid salt contents on proton conductivity of final product were discussed.

2. EXPERIMENTAL DETAILS

2.1. Preparation of PVA/Acid Salt Polymer Electrolytes

Poly(vinyl alcohol) PVA (degree of hydrolyzation $\geq 98\%$, $M_w = 72,000$), magnesium bromide MgBr_2 and phosphoric acid (H_3PO_4) were received from Sigma. The complex electrolytes were prepared by mixing of 0.4% (w/v) hydroquinone, 1% (w/v) ethylene carbonate PVA, MgBr_2 and H_3PO_4 at several stoichiometric ratios in distilled water to get $\text{PVA}_{(1-x)}(\text{MgBr}_2)_{x/2}(\text{H}_3\text{PO}_4)_{x/2}$ complex electrolytes, where x is 0.0, 0.1, 0.2, 0.3 and 0.4 Wt%. Solution with variable ratio was stirred vigorously and casted in Petri dish following solution cast technique at room temperature. Five different polymer electrolytes were produced.

2.2. Crystal Structure and Morphology Analysis

The crystalline structures of all the $\text{PVA}_{(1-x)}(\text{MgBr}_2)_{x/2}(\text{H}_3\text{PO}_4)_{x/2}$ composite polymer membranes were examined using a Philips X'Pert X-ray diffractometer (XRD) with

a Cu K_α radiation of wavelength $k = 1.54056 \text{ \AA}$ for 2θ angles between 4 and 60° .

The cross-sectional view and top surface morphologies and microstructures of all the complex electrolytes were examined with a S-2600H scanning electron microscope (Hitachi Co. Ltd.).

2.3. Ionic Conductivity and Transport Properties

Conductivity measurements were made for $\text{PVA}_{(1-x)}(\text{MgBr}_2)_{x/2}(\text{H}_3\text{PO}_4)_{x/2}$ composite polymer membrane by an ac impedance method. Samples of diameter 0.5 cm were sandwiched between the two similar brass electrodes of a spring-loaded sample holder. The whole assembly was placed in a furnace monitored by a temperature controller. The rate of heating was adjusted to be 2 K/min. Ionic and electronic transport numbers (t_{ion} , t_{ele}) were evaluated using Wagner's polarization technique. Impedance measurements were carried out in the temperature range 303–423 K using Hioki 3532 programmable automatic LCR meter. The measurements were carried out over a frequency range 100 Hz–100 kHz.

3. RESULTS AND DISCUSSION

3.1. Crystalline Structure and Surface Morphology

The X-ray diffraction measurement was performed to examine the nature of the crystallinity of the PVA/acid salt polymer electrolyte film. Figure 1 shows the diffraction pattern for the PVA polymer film and the composite PVA/acid salt polymer electrolyte film. It is well known that the PVA polymer film exhibits a semi-crystalline structure with peak at a 2θ angle of 20° . As can be seen clearly in Figure 1, a large peak at 2θ of 20° for the PVA polymer film was seen. But, it was also clearly seen that the peak intensity of the PVA/acid salt polymer electrolyte greatly reduced when the acid salt was added. This implies that the

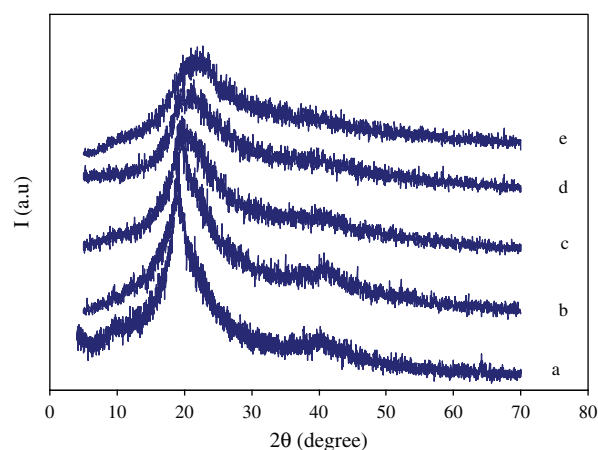


Fig. 1. The X-ray diffraction patterns of $\text{PVA}_{(1-x)}(\text{MgBr}_2)_{x/2}(\text{PWA})_{x/2}$ acid salt polymer electrolyte with (a) $x = 0.0$, (b) $x = 0.1$, (c) $x = 0.2$, (d) $x = 0.3$ and (e) $x = 0.4$.

addition of acid salt into PVA polymer matrix greatly augmented the domain of amorphous region (i.e., XRD crystal peak reduces). This indicates that the PVA/acid salt polymer electrolyte film becomes much amorphous. Notice that the degree of amorphous increases with increasing the contents of acid salt. There is a significant motion of polymer chain in the amorphous phase or some defects while non-conducting in the crystalline phase. The characteristic of the PVA/acid salt polymer electrolyte film shows excellent ionic conductivity property. This is due to the more free-volume and flexible of local PVA chain segmental motion in the PVA/acid salt polymer electrolyte.^(22–24)

The morphology of the free acid salt polymer electrolyte ($x = 0$) and composite PVA/acid salt polymer electrolyte film (with $0 \leq x < 0.4$) has been examined by SEM, and the images are shown in Figure 2. The free acid salt polymer electrolyte film is observed to have uniform, a homogeneous and dense material, Figure 2(a). The small amount of acid salt ($x = 0.1$) composite polymer electrolyte film is observed to have uniform small pores at microscopic level Figure 2(b). In the composite acid salt polymer electrolyte ($x = 0.2$), slightly larger in size and uniformly distributed pores are observed Figure 2(c). The uniformly dispersed pores in the polymer microstructure lead to the retention of liquid electrolyte and formation of their better connectivity through the polymer, giving rise to have possibility of high ionic conductivity.

3.2. Transference Number Measurement

The transference numbers corresponding to ionic (t_{ion}) and electronic (t_{elec}) transport have been calculated for

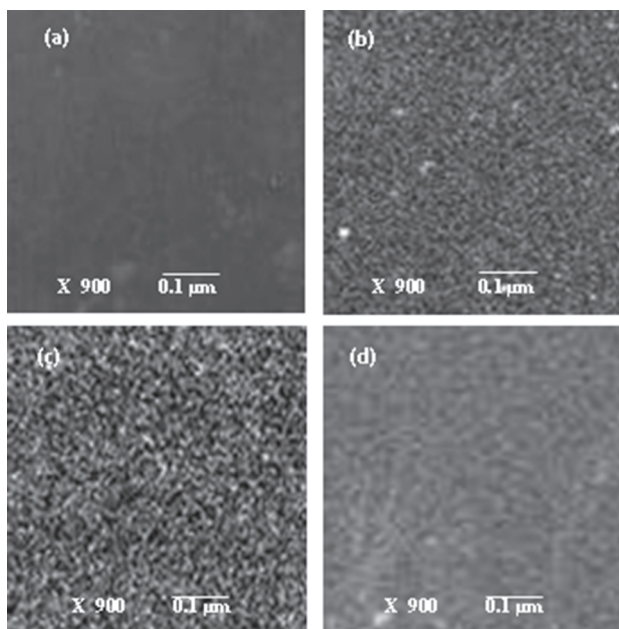


Fig. 2. The SEM micrograph for the surface of $PVA_{(1-x)}(MgBr_2)_{x/2}(H_3PO_4)_{x/2}$ solid acid salt polymer electrolyte with (a) $x = 0.0$, (b) $x = 0.1$, (c) $x = 0.2$, and (d) $x = 0.3$.

all compositions of PVA/acid salt polymer electrolyte systems using dc polarization method. In this method, the dc current is monitored as a function of time on the application of fixed dc voltage (1.5 V) across the sample with copper blocking electrodes. When acid salt increases, the pores size increases (Fig. 2(d)). Figure 3 shows the result of dc polarization measurements at 30 °C for $(PVA)_{0.6}(MgBr_2)_{0.2}(H_3PO_4)_{0.2}$ membrane. The transference numbers have been calculated from the polarization current versus time plot using the standard equation⁽²⁵⁾

$$t_{ion} = \frac{I_i - I_f}{I_i} \quad (1)$$

where I_i is the initial current and I_f is the final residual current. The ionic transference number (t_{ion}) for the composition of the ($x = 40$ wt%) electrolyte systems lies between 0.93 and 0.96. This suggests that the charge transport in these electrolyte films is predominantly ions.

3.3. Temperature Dependence of Ionic Conductivity

Impedance spectroscopy Figures 4(a), (b) shows the Cole-Cole plots of Z' versus Z'' (where Z' and Z'' are the real and imaginary parts of the complex impedance, respectively) of pure PVA and various compositions of complexed films with acid salt at different temperatures and different frequencies. These plots are single semicircular arcs with their centre's laying below the real axis at an angle θ . The finite value of distribution parameter θ and a depressed arc are typical for a material with multirelaxation processes.⁽²⁶⁾ Also, the arcs have a non-zero intersection with the real axis in the high frequency region. Further, there occurs a reduction in the size of these plots with rise in temperature and acid salt contents. The semi-circle represents the bulk conductivity, which is due to the

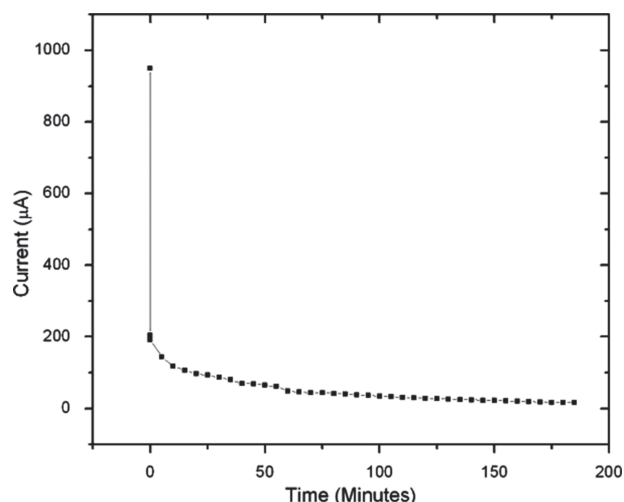


Fig. 3. Polarization current as a function of time for $x = 0.4$ PVA/acid salt polymer electrolyte.

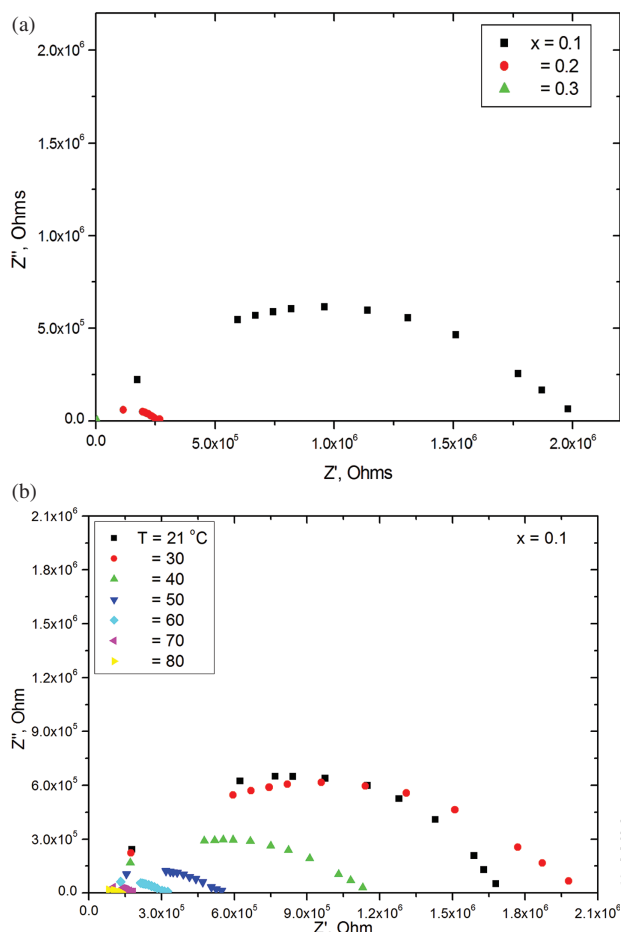


Fig. 4. Complex impedance plots of PVA_(1-x)(MgBr₂)_{x/2}(PWA)_{x/2} acid salt polymer electrolyte (a) different acid salt concentration at 303 K and (b) different temperatures ($x = 0.1$).

parallel combination of bulk resistance and bulk capacitance of the polymer electrolytes. Considering the equivalent circuit model, the values of Z' and Z'' are given by

$$Z' = R_s + \frac{R_p}{(1 + \omega^2 C_p^2 R_p^2)} \quad \text{and} \quad Z'' = \frac{-\omega C_p R_p^2}{1 + \omega^2 C_p^2 R_p^2} \quad (2)$$

where, R_s , R_p and C_p are the series resistor, parallel resistor and parallel capacitor respectively. Where $\omega = 2\pi f$ is the angular frequency.

These equations predict that the values of Z' and Z'' should decrease with increasing temperature as the values of R_p and R_s go on decreasing with rise in temperature in accordance with equation $C = C_p + 1/(\omega^2 R_p^2 C_p^2)$.

This causes shrinking of the Cole–Cole plots with increase in temperature and acid salt contents.

Singh et al.⁽²⁷⁾ have studied the relaxation characteristics of PVA-H₃PO₄ and PVA-H₂SO₄ complex electrolytes in the form of thin films samples and observed the impedance spectra as depressed single semicircular arcs for different samples corresponding to their two types of relaxation processes which are interpreted in terms of dipole-segmental

motion (α -relaxation) and side chain dipole group motion (β -relaxation). These results suggest that the migration of charges (ions) may occur through the free volume of matrix polymer, which can be represented by a resistor. On the other hand, non-migration charges (chains of polymer) polarized and can be therefore represented by a capacitor. The decrease in resistance of the polymer electrolyte is due to the enhancement of the ionic mobility and the number of carrier ions with acid salt concentration and temperature.⁽²⁸⁾

The bulk electrical resistance (R_b) of the material is obtained from the Cole–Cole plots with the intercept of the high frequency side on the X-axis. Analysis of the spectra yields information about the properties of the PVA/acid salt polymer electrolyte, such as bulk resistance, R_b . Taking into account the thickness of the PVA/acid salt electrolyte films, the R_b value was converted into the ionic conductivity value, σ , according to the formula:

$$\sigma = \frac{L}{R_b A} \quad (3)$$

where L is the thickness (cm) of the PVA/acid salt polymer electrolyte, A the area of the blocking electrode (cm²), and R_b is the bulk resistance (Ω) of PVA/acid salt polymer electrolyte.

Figure 5 shows the ionic conductivity values for the PVA/acid salt polymer electrolytes with different contents of acid salt. It can be seen clearly that the ionic conductivity of the PVA/acid salt SPE can be significantly enhanced when the content of acid salt increases.

Figure 6 represents the temperature dependence of ionic conductivity for all compositions of PVA_(1-x)(MgBr₂)_{x/2}(H₃PO₄)_{x/2} polymer electrolytes. It has been found that the ionic conductivity of the PVA/acid salt SPE increases with increasing temperature for all compositions, indicating

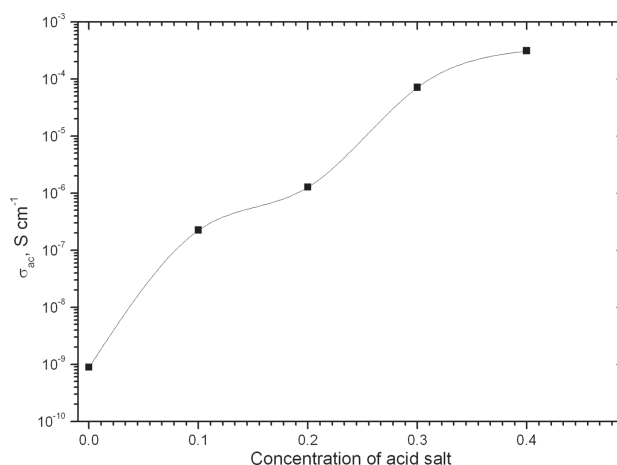


Fig. 5. The Influence of acid salt content on ionic conductivity of PVA_(1-x)(MgBr₂)_{x/2}(H₃PO₄)_{x/2} solid acid salt polymer electrolyte.

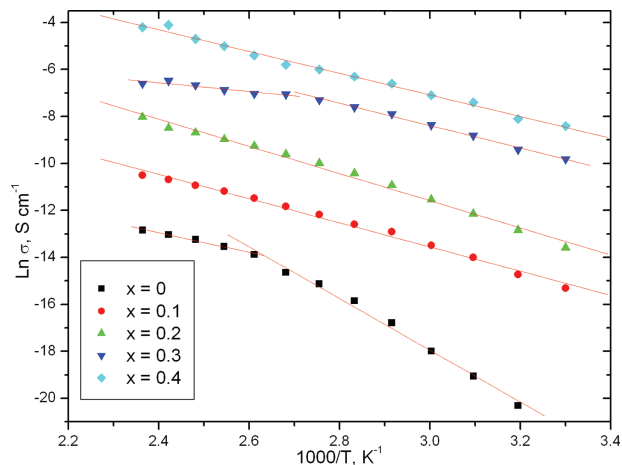


Fig. 6. Arrhenius plot for PVA_(1-x)(MgBr₂)_{x/2}(H₃PO₄)_{x/2} solid acid salt polymer electrolyte.

Arrhenius type thermally activated process given by the relation

$$\sigma = \sigma_o \exp\left(-\frac{E_a}{RT}\right) \quad (4)$$

where σ_o is a pre-exponential factor, E_a the activation energy, and T is the temperature in Kelvin. This can be explained on the basis of the free volume model⁽²⁹⁾ and hopping of charge carriers between the localized states.⁽³⁰⁾ Since poly(vinyl alcohol) is a linear polymer with carbon chain as the back bone, the polymer chains which are less entangled are capable of causing electrical conductivity.

Further PVA being a polar polymer, ionizes the MgBr₂ salt into anions and cations under the influence of the applied electric field and temperature. These ions hop between the localized states and cause enhanced conductivity. Further, when the temperature is increased, the vibration energy of a segmental is sufficient to push against the hydrostatic pressure imposed by its neighboring atoms and create a small amount of space surrounding its own volume in which vibration motion can occur.⁽³¹⁾ Therefore, the free volume around the polymer chain causes the mobility of ions and polymer segments and hence, the conductivity. The increment of temperature causes the increase in conductivity due to the increased free volume and their respective ionic and segmental mobility. The amorphous

Table I. Effect of the acid salt concentration on the activation energies (E_a) and conduction index (n) values.

Acid salt (x)	Energy		Conduction index n
	Region I	Region II	
0.0	0.78	0.36	1.46
0.1	0.52	–	0.49
0.2	0.58	–	0.17
0.3	0.39	0.26	0.04
0.4	0.38	–	0.07

nature also provides a bigger free volume in the polymer electrolytes system upon increasing temperature.⁽³²⁾ The $\ln(\sigma)$ versus $10^3/T$ plots obtains the activation energy (E_a) of the PVA/acid salt SPE, which is dependent on the contents of acid salt in the polymer matrix.

It has been found that the highest conductivity polymer electrolyte ($x = 0.4$) has the lowest activation energy (0.38 eV), see Table I. It is noteworthy that the polymer electrolytes with low values of activation energies are desirable for practical applications.

Figure 7 shows the frequency-dependent conductivity of PVA_(1-x)(MgBr₂)_{x/2}(H₃PO₄)_{x/2} polymer electrolytes. The plot shows two regions: The first region observed at low frequency plateau region corresponds to the frequency independent conductivity (σ_{dc}). The second region observed at the high frequency dispersion region which corresponds to the conductivity increases with increasing frequency. This behavior obeys the universal power law⁽¹³⁾

$$\sigma_{tot}(\omega) = \sigma_{dc} + A\omega^n \quad (5)$$

where σ_{dc} is the dc conductivity (the extrapolation of the plateau region to zero frequency), A is the pre-exponential factor, ω is the angular frequency and n the fractional exponent which lies between 0 and 1. According to the jump relaxation model, at low frequencies, ions can jump from one site to its neighboring site. While at higher frequencies, due to the short time periods, the probability for ions to go back to their initial sites increases which causes increase in the conductivity.^(33,34) The values of the exponent n have been obtained using the least square fitting of Eq. (5); it can be observed that the exponent n decreases with increasing concentration of the acid salt, see Table I. This behavior can be interpreted in light of the fact that doping of acid salt increases the number of chain segments that are responsive to the external electric field frequency.

The study of dielectric relaxation in solid polymer electrolytes is a powerful approach for obtaining information

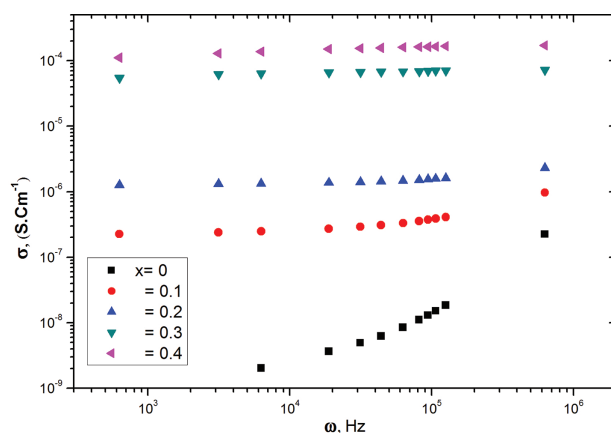


Fig. 7. Conductivity-frequency dependence plot for PVA_(1-x)(MgBr₂)_{x/2}(H₃PO₄)_{x/2} solid acid salt polymer electrolyte.

about the characteristics of ionic and molecular interactions. The dielectric parameters associated with relaxation processes are of particular significance in ion conducting polymers where the dielectric constant plays a fundamental role which shows the ability of a polymer material to dissolve salts.

The dielectric constant was used as an indicator to show that the increase in conductivity is mainly due to an increase in the number density of mobile ions.⁽³⁵⁾ The relationship between complex impedance, dielectric permittivity and dielectric loss can be shown in the following formulae: $\varepsilon' = (C_p L) / (\varepsilon_o A)$, $\varepsilon'' = \sigma / (\omega \varepsilon_o)$, where ε' denotes the real part of dielectric function, ε'' as the imaginary part of dielectric function or dielectric loss and ε_o as the permittivity of the free space. Figures 8(a), (b) shows the variation of the dielectric permittivity ε' and dielectric loss ε'' , for PVA_(1-x)(MgBr₂)_{x/2}(H₃PO₄)_{x/2} polymer electrolytes versus frequency at room temperature, 30 °C. The figure show that ε' and ε'' a gradually decrease with increasing frequency for all prepared samples. The decrease of ε' and ε'' with frequency can be associated to the inability of dipoles to rotate rapidly leading to a lag between frequency of oscillating dipole and

that of applied field. The variation indicates that at low frequencies the dielectric constant is high due to the interfacial polarization and the dielectric loss (ε'') becomes very large at lower frequencies due to free charge motion within the material.⁽³⁶⁾

This behavior can be described by the Debye dispersion relation,⁽³⁷⁾

$$\varepsilon' \cong \varepsilon_\infty + \frac{\varepsilon_s - \varepsilon_\infty}{1 + \omega^2 \tau^2}, \quad \varepsilon'' \cong \frac{(\varepsilon_s - \varepsilon_\infty) \omega \tau}{1 + \omega^2 \tau^2} \quad (6)$$

where ε_∞ and ε_s are the static and infinite dielectric permittivity, τ is the relaxation time and ω is the angular frequency.

Figures 9(a)–(b) show the variation of dielectric permittivity ε' and dielectric loss ε'' for PVA_(1-x)(MgBr₂)_{x/2}(H₃PO₄)_{x/2} polymer electrolytes with temperature at 1 kHz. The value of ε' and ε'' increases with temperature. The observed increase in of ε' and dielectric loss ε'' with temperature could be attributed to decrease in the viscosity of the polymeric material. This leads to an increment in the degree of dipole orientation of polar dielectric material and hence dielectric constant

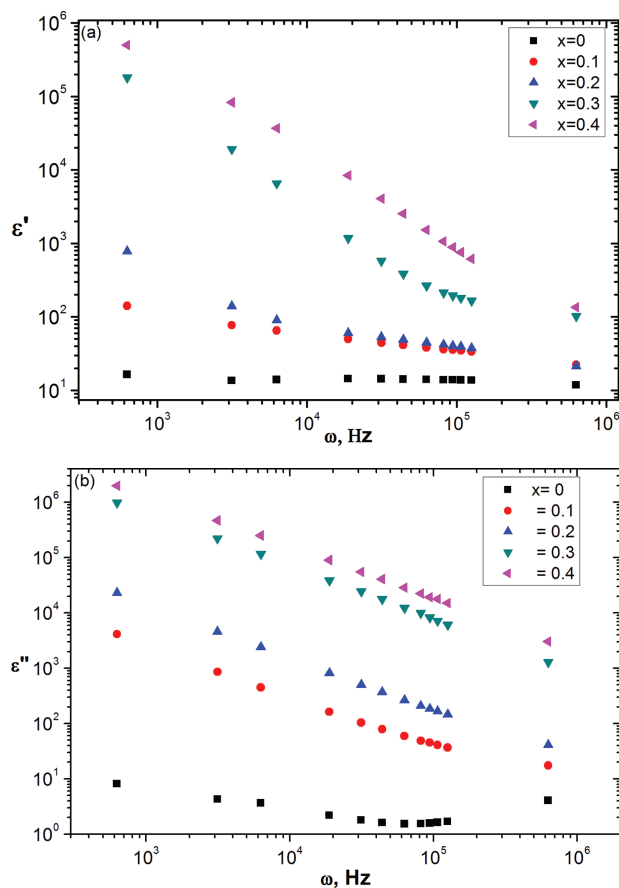


Fig. 8. Frequency dependence of (a) Dielectric constant ε' , and (b) dielectric loss ε'' for PVA_(1-x)(MgBr₂)_{x/2}(H₃PO₄)_{x/2} solid acid salt polymer electrolyte.

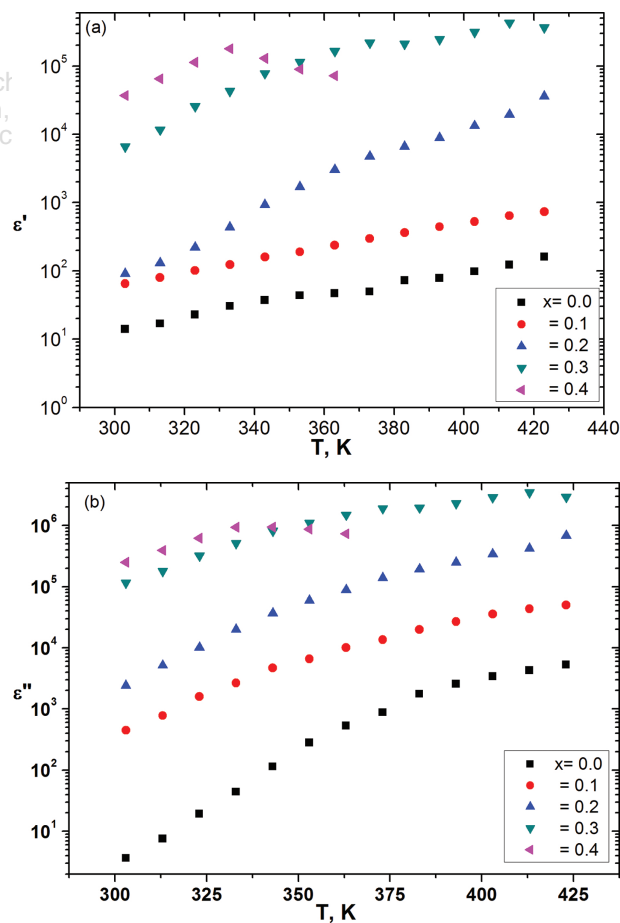


Fig. 9. Temperature dependence of (a) Dielectric constant ε' , and (b) dielectric loss ε'' for PVA_(1-x)(MgBr₂)_{x/2}(H₃PO₄)_{x/2} solid acid salt polymer electrolyte.

increases.⁽³⁸⁾ Dipolar molecules should be able to orient from one equilibrium position to another relatively easily, and contribute to absorption.⁽³⁹⁾

4. CONCLUSION

PVA/acid salt polymer electrolytes with a different composition were obtained by a solution casting method. The physico-chemical characteristic properties of the composite are systematically studied by using a XRD, SEM, and AC impedance method. The XRD study reveals the amorphous nature of the polymer-acid salt complexes that produces high ionic diffusivity. The introduction of acid salt to the PVA polymer electrolytes has proved to be a convenient method to increase the ionic conductivity at ambient temperature. Addition of acid salt causes an enhancement in its mobility and charge carrier concentration. The ionic transference number of mobile ions has been estimated to be in the range 0.93 and 0.96 revealing that the conducting species are predominantly due to ions. The temperature dependence of conductivity of PVA/acid salt obeys Arrhenius relation in the temperature range studied. In fact, the ionic conductivity value greatly depends on the acid salt contents in the PVA polymer electrolyte. These composite PVA/acid salt polymer electrolytes show a highly potential for applications on fuel cell systems.

Acknowledgment: The financial supported for this study from the University of Tabuk, Saudi Arabia under the project No. 21/21/1432H are gratefully acknowledged.

References and Notes

- J. Lee, Y. Lee, W. Chae, and Y. Sung; Enhanced ionic conductivity in PEO-LiClO₄ hybrid electrolytes by structural modification; *J. Electroceram.* 17, 941 (2006).
- M. Sundar and S. Selladurai; Effect of fillers on Magnesium-poly(ethylene oxide) solid polymer electrolyte; *Ionics* 12, 281 (2006).
- V. Subba Reddy Ch, A. P. Jin, Q. Y. Zhu, L. Q. Mai, and W. Chen; Preparation and characterization of (PVP + NaClO₄) electrolytes for battery applications; *Eur. Phys. J. E Soft Matter.* 19, 471 (2006).
- M. B. Armand; Polymer electrolytes; *Ann. Rev. Mater. Sci.* 16, 245 (1986).
- J. R. MacCullum and C. A. Vincent; Polymer Electrolytes Reviews, Elsevier Applied Science Publisher, London (1987) and (1989), Vols. 1–2.
- D. E. Fenton, J. M. Parker, and P. V. Wright; Complexes of alkali metal ions with poly(ethylene oxide); *Polymer* 14, 589 (1973).
- C. W. Walker Jr and M. Salomon; Improvement of ionic conductivity in plasticized PEO-based solid polymer electrolytes; *J. Electrochem. Soc.* 140, 3409 (1993).
- C. A. Finch; Polyvinylalcohol, Wiley Interscience Pub, New York (1973).
- F. Ahmad and E. Sheha; Preparation and physical properties of (PVA)_{0.7}(NaBr)_{0.3}(H₃PO₄)_{xM} solid acid membrane for phosphoric acid—Fuel cells; *J. Advanced Research* 4, 155 (2013).
- T. Dippel, K. D. Kreuer, J. C. Lassègues, and D. Rodriguez; Proton conductivity in fused phosphoric acid: A ¹H/³¹P PFG-NMR and QNS study; *Solid State Ionics* 61, 41 (1993).
- S. Ü. Çelik, A. Aslan, and A. Bozkurt; Phosphoric acid-doped poly(1-vinyl-1,2,4-triazole) as water-free proton conducting polymer electrolytes; *Solid State Ionics* 179, 683 (2008).
- P. Donoso, W. Gorecki, C. Berthier, F. Defendini, C. Poinson, and M. B. Armand; NMR, conductivity and neutron scattering investigation of ionic dynamics in the anhydrous polymer protonic conductor PEO(H₃PO₄)_x; *Solid State Ionics* 28–30, 969 (1988).
- E. Sheha; Preparation and physical properties of (PVA)_{0.75}(NH₄Br)_{0.25}(H₂SO₄)_{xM} solid acid membrane; *Journal of Non-Crystalline Solids* 356, 2282 (2010).
- A. Aslan, S. Ü. Çelik, and A. Bozkurt; Proton-conducting properties of the membranes based on poly(vinyl phosphonic acid) grafted poly(glycidyl methacrylate); *Solid State Ionics* 180, 1240 (2009).
- M. F. Daniel, B. Desbat, F. Cruege, O. Trinquet, and J. C. Lassegues; Solid state protonic conductors: Poly(ethyleneimine) sulfates and phosphates; *Solid State Ionics* 28–30, 637 (1988).
- R. Tanaka, H. Yamamoto, A. Shono, K. Kubo, and M. Sakurai; Proton conducting behavior in non-crosslinked and crosslinked polyethylenimine with excess phosphoric acid; *Electrochim Acta* 45, 1385 (2000).
- S. R. Samms, S. Wasmus, and R. F. Savinell; Thermal stability of proton conducting acid doped Polybenzimidazole in simulated fuel cell Environments. *J. Electrochem Soc.* 143, 1225 (1996).
- Q. Li, R. He, J.-A. Gao, J. O. Jensen, and N. J. Bjerrum; The CO poisoning effect in PEMFCs operational at temperatures up to 200 °C; *J. Electrochem Soc.* 150, A1599 (2003).
- H. Pu, W. H. Meyer, and G. Wegner; Proton transport in polybenzimidazole blended with H₃PO₄ or H₂SO₄; *J. Polymer Sci. B Polymer Phys.* 40, 663 (2002).
- Y. Zhai, H. Zhang, Y. Zhang, and D. Xing; A novel H₃PO₄/Nafion-PBI composite membrane for enhanced durability of high temperature PEM fuel cells; *J. Power Source* 169, 259 (2007).
- B. Samy and E. Sheha; Impact of hydroquinone on thermal and electrical properties of plasticized [poly(vinylalcohol)]_{0.7}(LiBr)_{0.3}(H₂SO₄)_{2.5 molL}⁻¹ solid acid membrane; *Polymer Int.* 60, 1142 (2011).
- A. Hassen, T. Hanafy, S. El. Sayed, and A. Himanshu; Dielectric relaxation and alternating current conductivity of polyvinylidene fluoride doped with lanthanum chloride; *J. Appl. Physics* 110, 114 (2011).
- S. Mahrous and T. Hanafy; Dielectric analysis of chlorinated polyvinyl chloride stabilized with di-n-octyltin maleate; *J. Applied Polymer Science* 113, 316 (2009).
- B. Wagner and C. Wagner; Electrical conductivity measurements on cuprous halides; *J. Chem. Phys.* 26, 1597 (1957).
- M. Hema, S. Selvasekerapandian, A. Sakunthala, D. Arunkumar, and H. Nithy; Structural, vibrational and electrical characterization of PVA–NH₄Br polymer electrolyte system; *Physica B* 403, 2740 (2008).
- E. Barsoukov and J. Ross Macdonald; Impedance Spectroscopy: Theory, Experiment, and Applications-Wiley-Interscience (2005).
- K. P. Singh and P. N. Gupta; Study of dielectric relaxation in polymer electrolytes; *Eur. Polym. J.* 34, 1023 (1998).
- R. Baskaran, S. Selvasekharapandian, H. Kumar, and G. Bhuvanewari; Dielectric and conductivity relaxations in PVAc based; *Ionics* 10, 129 (2004).
- J. R. Chetia, M. Maullick, A. Dutta, and N. N. Dass; Role of poly(2-dimethylaminoethylmethacrylate) salt as solid state ionics; *Mater. Sci. Eng. B* 107, 134 (2004).
- P. K. C. Pillai, P. Khurana, and A. Trilateral; Dielectric studies of poly(methyl methacrylate)/polystyrene double layer system; *J. Mat. Sci. Lett.* 5, 629 (1986).
- M. S. Michael, M. E. Jacob, S. Prabaharan, and S. Radhakrishna; Enhanced lithium ion transport in PEO-based solid polymer electrolytes employing a novel class of plasticizers; *Solid State Ionics* 98, 167 (1997).
- A. K. Jonscher; The ‘universal’ dielectric response; *Nature* 267, 673 (1977).
- M. Ahmad, S. H. Sabeeh, and S. A. Hussien; Electrical and optical properties of PVA/LiI polymer electrolyte films; *Asian Transactions on Science & Technology* 1, 16 (2012).

34. E. Sheha and M. K. El-Mansy; A high voltage magnesium battery based on H₂SO₄-doped (PVA)_{0.7}(NaBr)_{0.3} solid polymer electrolyte; *J. Power Sources* 185, 1509 (2008).
35. S. R. Majid and A. K. Arof; Electrical behavior of proton-conducting chitosan-phosphoric acid-based electrolytes; *Physica B* 390, 209 (2007).
36. A. Kyritsis, P. Pissis, and J. Grammatikakis; Dielectric relaxation spectroscopy in poly(hydroxyethyl acrylates)/water hydrogels; *J. Polymer Sci., Part B: Polymer Phys.* 33, 1737 (1995).
37. E. Nora; Dielectric Properties and Molecular Behavior, Series in Physical Chemistry Publishers, Van Nostrand (1969).
38. G. K. Prajapati, R. Roshan, and P. N. Gupta; Effect of plasticizer on ionic transport and dielectric properties of PVA-H₃PO₄ proton conducting polymeric electrolytes; *J. Phys. Chem. Solids* 71, 1717 (2010).
39. E. Sheha; Ionic conductivity and dielectric properties of plasticized PVA_{0.7}(LiBr)_{0.3}(H₂SO₄)_{2.7 M} solid acid membrane and its performance in a magnesium battery; *Solid State Ionics* 180, 1575 (2009).

Received: 1 July 2014. Revised/Accepted: 24 August 2014.

Delivered by Publishing Technology to: Guest User
IP: 193.227.36.253 On: Sun, 28 Dec 2014 13:18:04
Copyright: American Scientific Publishers